1.0 ⊢ 2.8 2.5
4.5
5.0
5.5
1.1 3.2 2.2
3.6
4.0 2.0
1.8
1.25 1.4 1.6

MICROCOPY RESOLUTION TEST CHART
NATIONAL BUREAU OF STANDARDS-1963

REPORT DOCUMENTATION PAGE

1a. REPORT SECURITY CLASSIFICATION UNCLASSIFIED	1b. RESTRICTIVE MARKINGS

	3. DISTRIBUTION/AVAILABILITY OF REPORT Approved for public release, distribution unlimited UNCLASSIFIED, UNLIMITED
AD-A179 582 s)	5. MONITORING ORGANIZATION REPORT NUMBER(S) AFOSR·TR· 87-0389

6a. NAME OF PERFORMING ORGANIZATION University of Arizona	6b. OFFICE SYMBOL (If applicable) N/A	7a. NAME OF MONITORING ORGANIZATION Air Force Office of Scientific Research
6c. ADDRESS (City, State and ZIP Code) Engineering Experiment Station College of Engineering & Mines Tucson, AZ 85721		7b. ADDRESS (City, State and ZIP Code) Bolling Air Force Base, Building 410 Washington, DC 20332

8a. NAME OF FUNDING/SPONSORING ORGANIZATION Air Force Office of Scientific Research	8b. OFFICE SYMBOL (If applicable) AFSC	9. PROCUREMENT INSTRUMENT IDENTIFICATION NUMBER AFOSR-84-0054

8c. ADDRESS (City, State and ZIP Code) Bolling Air Force Base Building 410 Washington, DC 20332	10. SOURCE OF FUNDING NOS.			
	PROGRAM ELEMENT NO. 61102F	PROJECT NO. 2307	TASK NO. A2	WORK UNIT NO.

11. TITLE (Include Security Classification)
THE STRUCTURE OF TURBULENT VELOCITY FIELDS

12. PERSONAL AUTHOR(S)
F. H. Champagne

13a. TYPE OF REPORT FINAL	13b. TIME COVERED FROM 2/1/84 TO 1/31/85	14. DATE OF REPORT (Yr., Mo., Day) 1/24/86	15. PAGE COUNT 23

16. SUPPLEMENTARY NOTATION

17.	COSATI CODES		18. SUBJECT TERMS (Continue on reverse if necessary and identify by block number)
FIELD	GROUP	SUB. GR.	
			TURBULENCE, WAKES, COHERENT STRUCTURES, MODES

19. ABSTRACT (Continue on reverse if necessary and identify by block number)

Sinusoidal disturbances, symmetrically distributed about the centerline of a turbulent wake, were introduced near the trailing edge of a flat plate to generate the varicose mode of instability. Phase-averaged measurements of the u-component of velocity fluctuations were decomposed into the two modes, and the results were compared with the appropriate theoretical eigenfunctions. The later distribution of the amplitude and phase of each mode agree reasonably well with their theoretical counterparts. The amplitude ratio of the two modes appear to approach an asymptitic value in the far wake. Keywords:,

DTIC ELECTED
APR 2 8 1987
S E

20. DISTRIBUTION/AVAILABILITY OF ABSTRACT UNCLASSIFIED/UNLIMITED ☐ SAME AS RPT. ☒ DTIC USERS ☐	21. ABSTRACT SECURITY CLASSIFICATION UNCLASSIFIED
22a. NAME OF RESPONSIBLE INDIVIDUAL Henry E Helin	22b. TELEPHONE NUMBER (Include Area Code) 202 767 4935	22c. OFFICE SYMBOL AFOSR/NA

DD FORM 1473, 83 APR   EDITION OF 1 JAN 73 IS OBSOLETE.   UNCLASSIFIED

TABLE OF CONTENTS

Accession For	
NTIS GRA&I	☑
DTIC TAB	☐
Unannounced	☐
Justification	

By	
Distribution/	
Availability Codes	
Dist	Avail and/or Special
A-1	

QUALITY INSPECTED 1

INTRODUCTION

The contract AFOSR-84-0054 was for a one year period, and a 'bare bones' budget of $46,994 was awarded. Some significant work was completed during this period which severed as a basis for a presentation at the 1984 APS Division of Fluid Dynamics Meeting. A brief description of the work is as follows.

In the previous final report, we presented results from experiments where we externally imposed sinuous waves on a fully turbulent wake behind a flat plate. A manuscript based on these results has been accepted for publication by The Journal of Fluid Mechanics. We showed that although the sinuous disturbances represent the predominant mode of instability from linear stability theory, the varicose disturbances (those which are symmetrical about the wake centerline) may play a role in determining the nature of the large coherent structures observed in the far wake. Varicose disturbances have relatively smaller amplification rates and are usually neglected in a parallel flow analysis. The varicose mode, however, may at times dominate the shape of the large structures (Papailiuou and Lykoudis, 1974) and even when the prevailing instability is mainly sinuous in nature, a small varicose component was shown to alter the gross behavior of the calculated streakline patterns (see last years report). The latter provided the initial motivation for the current work which is to investigate the significance of the varicose mode in two-dimensional, small deficit turbulent wakes. It should be noted that the varicose mode has not been

investigated experimentally in either laminar or turbulent wakes and its existence was by no means assured, particularly in a fully turbulent environment.

GENERATION OF VARICOSE MODE

In this report, we will present the results of our attempts to force varicose waves. Sinusoidal disturbances, symmetrically distributed about the wake centerline, were generated by oscillating two small flaps 180° out of phase. The flaps were placed symmetrically above and below the flat plate, as indicated in Figure 1. It is extremely difficult to generate purely symmetrical disturbances because the spatial amplification rates for the varicose mode are as much as two orders of magnitude smaller than those for the sinuous mode. Any lack of symmetry in the generating mechanism resulted in a combination of modes. The results of one attempt to generate a pure varicose mode are given in Figure 2. Data on the lateral distributions of $\overline{u^2}/u_o^2$ for downstream location in the range $100 \leq x/\hat{\theta} \leq 1400$ are shown. The flaps were driven in phase at 35Hz and a rake of 9 hot wires was used to obtain the data. The data indicates that flow is self preserving, but the self preserving distribution for this case differs from that for the unforced case which is shown in Figure 3 for comparison. In particular, the ratio of $\overline{u^2}/\overline{u^2}_{max}$ in 0.76 for the unforced case and 0.80 for the forced case.

The mean velocity distributions for each wake are self preserving, although the wakes developed at different rates in the downstream
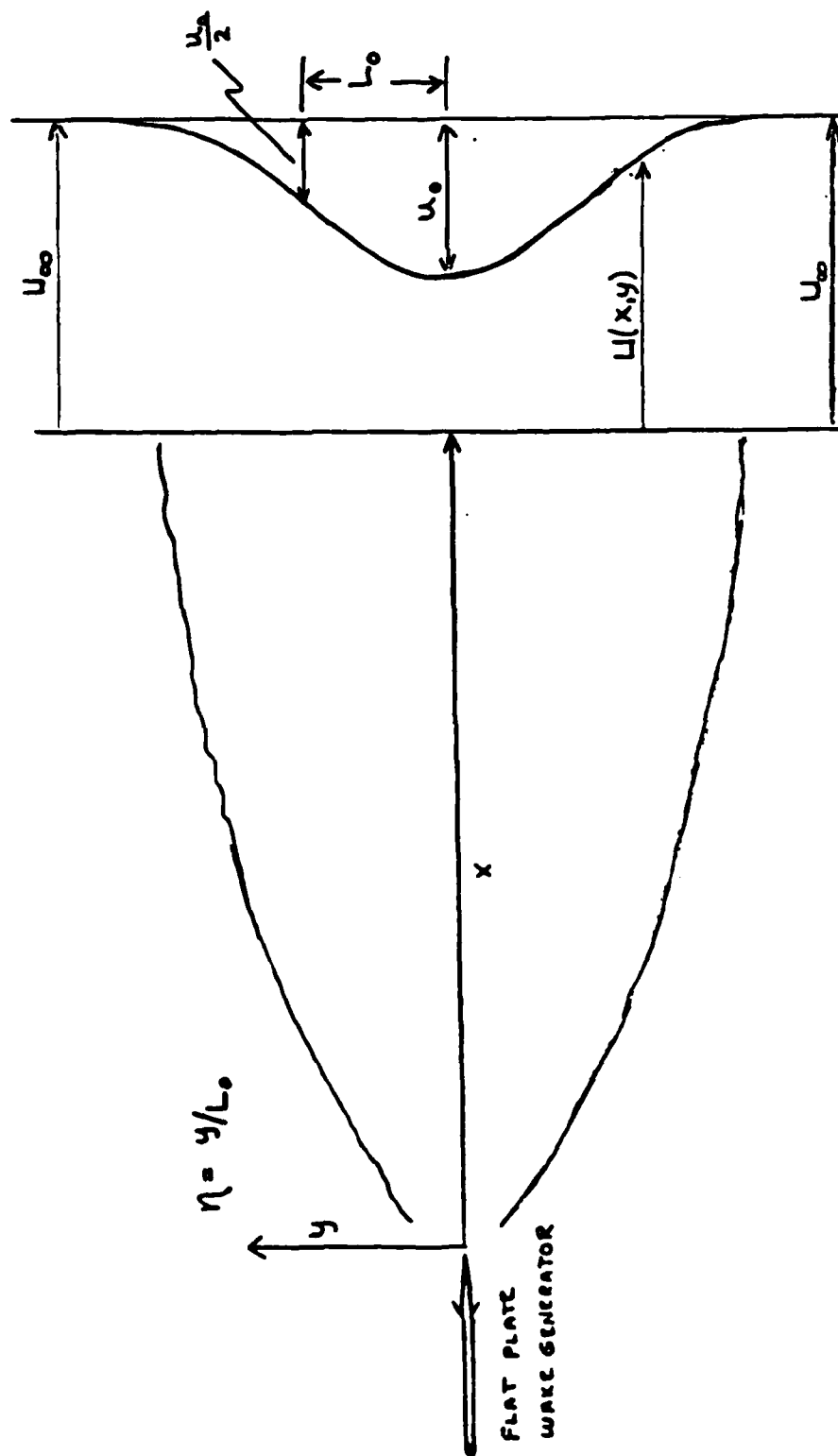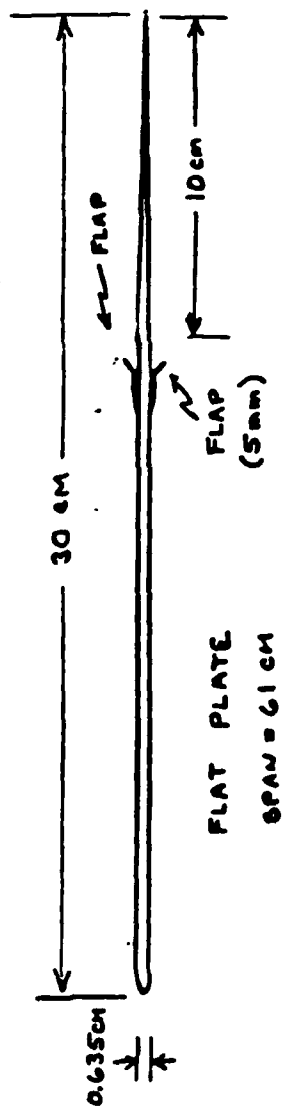
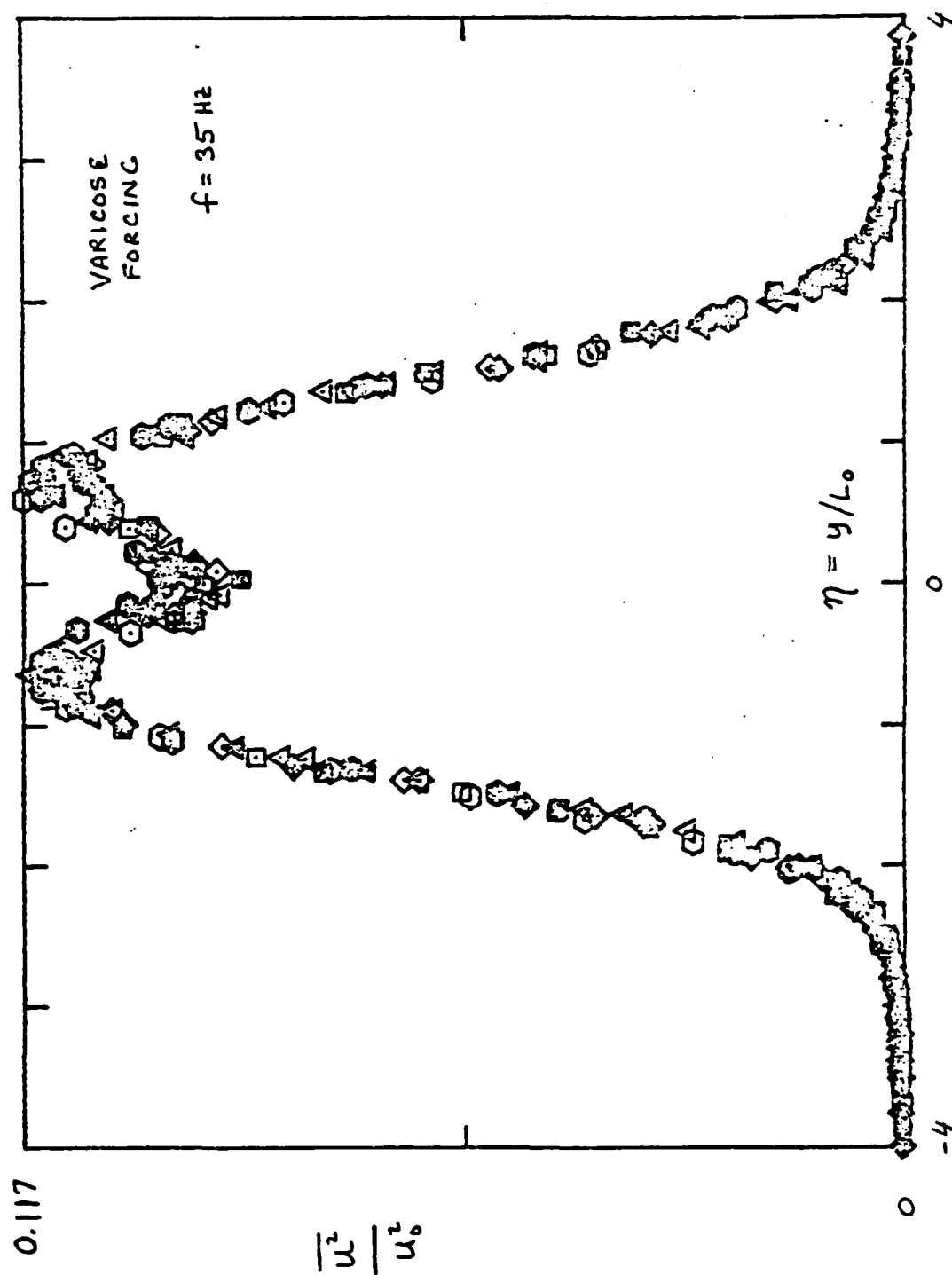FIGURE 1: Schematic of plate and wake defining the nomenclature

$\frac{U_o}{2}$

L_o

U_∞

U_o

$U(x,y)$

U_∞

x

$\eta = y/L_o$

y

FLAT PLATE
WAKE GENERATOR

FLAP

FLAP
(5mm)

10cm

30 cm

FLAT PLATE
SPAN = 61 CM

0.635cm

3

FIGURE 2: The measured distribution of $\overline{u^2}/u_o^2$ for the varicose forced wake. Different symbols represent different downstream locations in the range $100 < x/\ominus < 1400$.
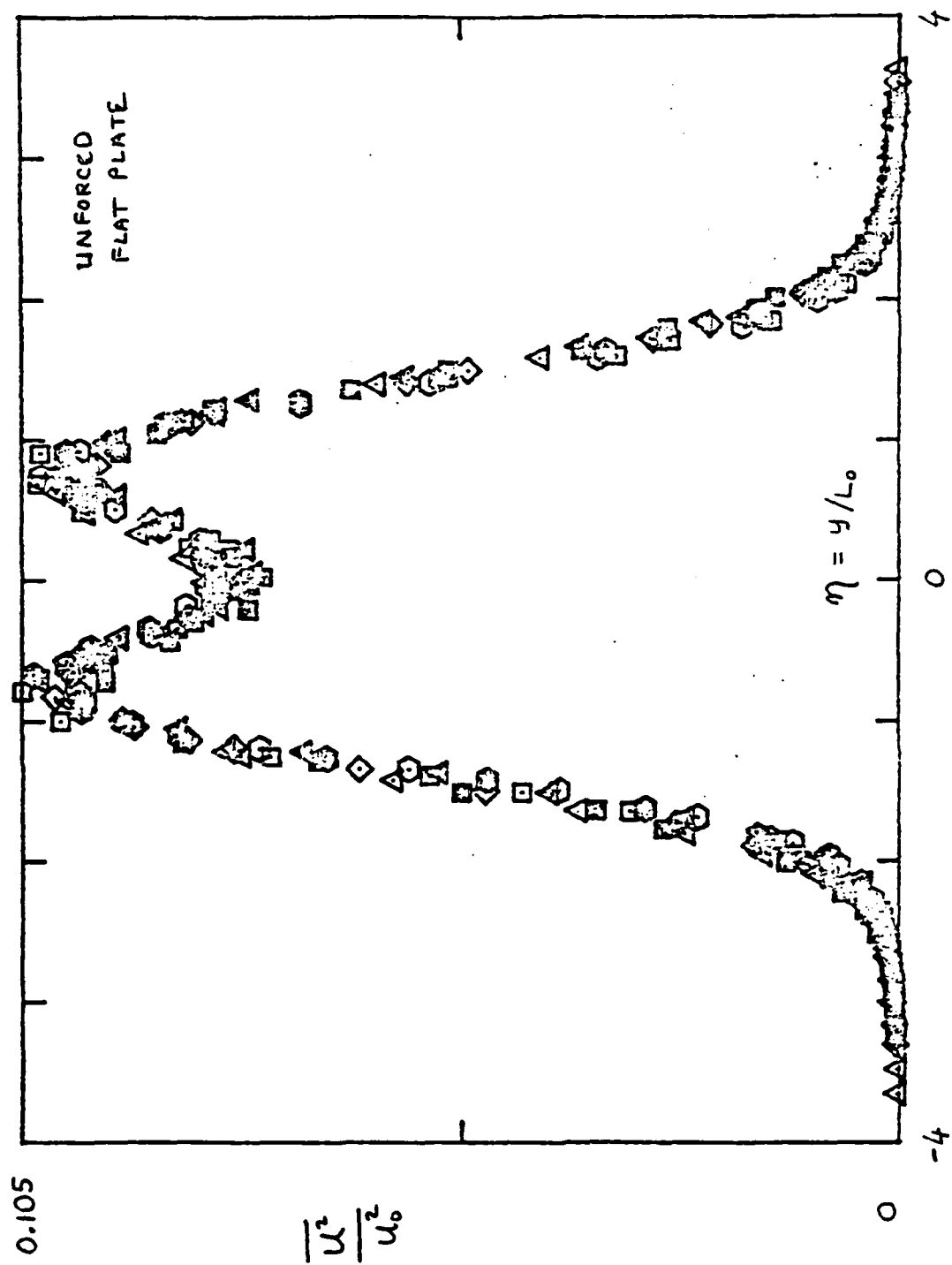
4

FIGURE 3: The measured distribution of $\overline{u^2}/u_o^2$ for the unfoced wake.

direction. The streamwise development of the characteristic scales u_o and L_o can be expressed as:

$$\left(\frac{U_\infty}{u_o}\right)^2 = \frac{x}{W_o^2 \, \Theta}$$

$$\left(\frac{L_o}{\Theta}\right)^2 = \Delta_o^2 \, \frac{x}{\Theta}$$

where W_o and Δ_o are constants for a given self preserving wake. The values of W_o and Δ_o for the unfoced wake are 1.68 and 0.304, respectively, while those for the varicose forced wake are 1.62 and 0.312, respectively. The mean field is therefore affected slightly by the forcing. The self preserving mean velocity profiles are, however, effectively identical for the two wakes. That is, plots of the self preserving function $f(\eta)$, defined by

$$f(\eta) = \frac{U_\infty - U(x,y)}{u_o(x)} \, ,$$

for the two wakes are identical to within the experimental uncertainty. Therefore, the mean and turbulent fields are affected by the forcing.

The distributions of the amplitudes and phases of the velocity perturbations associated with the varicose waves are shown in Figure 4(a) and 4(b) for five downstream locations. The data, shown by the symbols, were obtained by recording the velcotiy signal together with the sinusiodal signal activating the flaps. The velocity signal was phase averaged over 100 cycles of the flap motion and the Fourier transform provided the
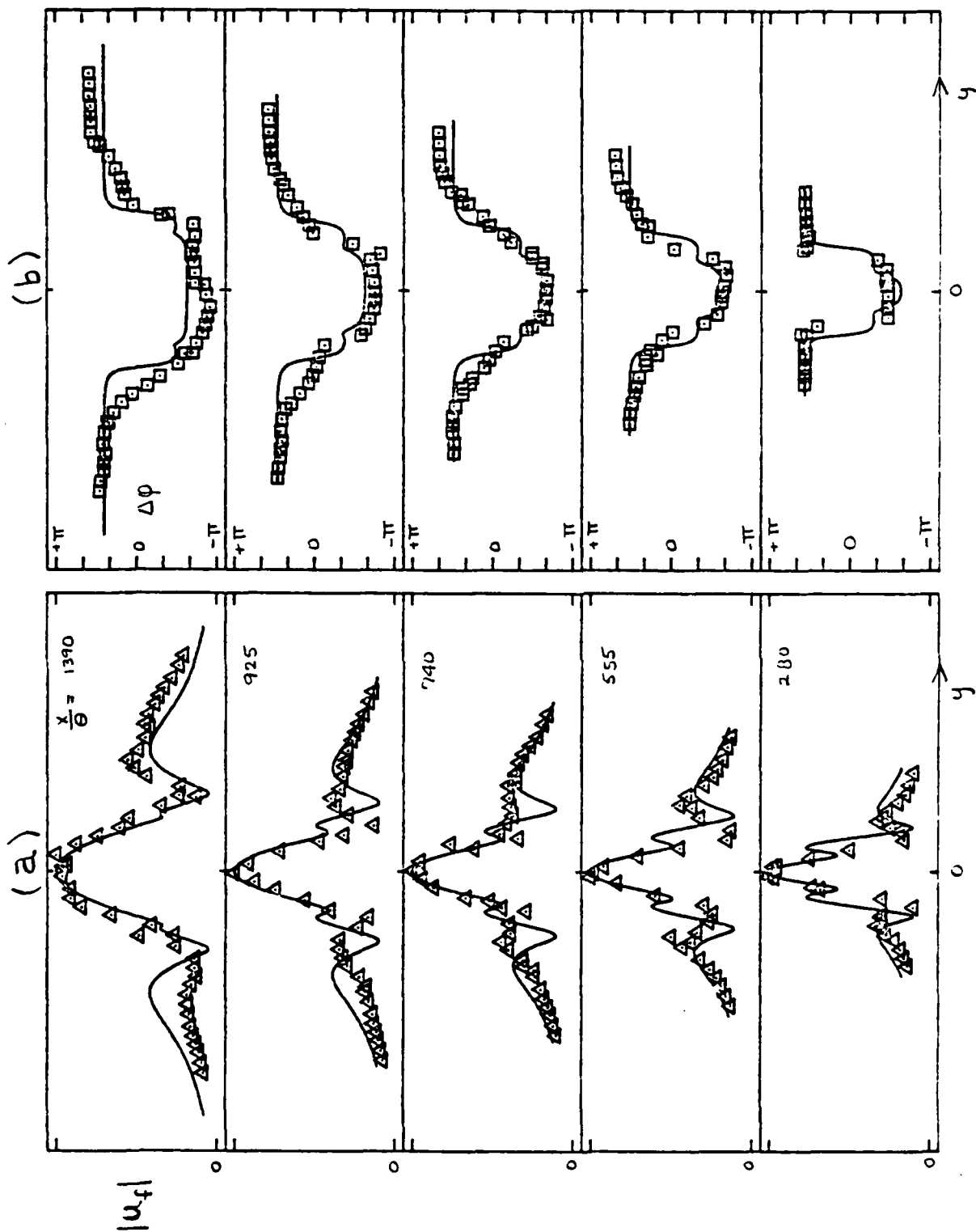
6

FIGURE 4(a): The distributions of the disturbance amplitude; Δ, phase averaged measurements; ——— theoretical varicose.

FIGURE 4(b): The distribution of the disturbance phase; □, phase averaged measurements; ——— theoretical varicose.

amplitudes and phase estimates of the spectral elements of the velocity field. The estimates were quite free from the random turbulent fluctuations present in the original signal. The absicca in both figures is dimensional y which covers the range $-4L_o < y < 4L_o$. The ordinate in Figure 4(a) is the amplitude u_f, the subscript f denoting the forcing frequency and in Figure 4(b) the ordinate is relative phase shift, $\Delta\phi$. The results are displayed to indicate the downstream evolution of the forced wave. The solid lines represent the theoretical results computed from linear stability theory using the measured mean velocity profiles. The theoretical amplitude is plotted versus y and the only adjustment is that the area under the theoretical curve is matched to that under the measured data. There is reasonable agreement between the experimental and theoretical results, although not quite as good as that obtained for the sinuous mode. Some of the fine details such as the minor lobes closest to the centerline shown in the theoretical curves are not evident in the experimental results. This is undoubtedly caused by viscous effects which would tend to eliminate such regions of high velocity gradient. (This will be investigated further by attempting to solve the Orr-Sommerfeld equation for the wake. See next year's report for results.) The maximum measured amplitude of the varicose wave at each downstream location is plotted versus x/Θ in Figure 5. It appears that the value of u_{max} is nearly constant in the far wake, but more data at larger x is required. At large x, a notable lack of symmetry sets in. This cannot be attributed to probe interference problems, but rather is caused by the presence of the sinuous mode. The difficulty encountered in generating a purely symmetric disturbance wave indicates the flow is very sensitive to even the slightest
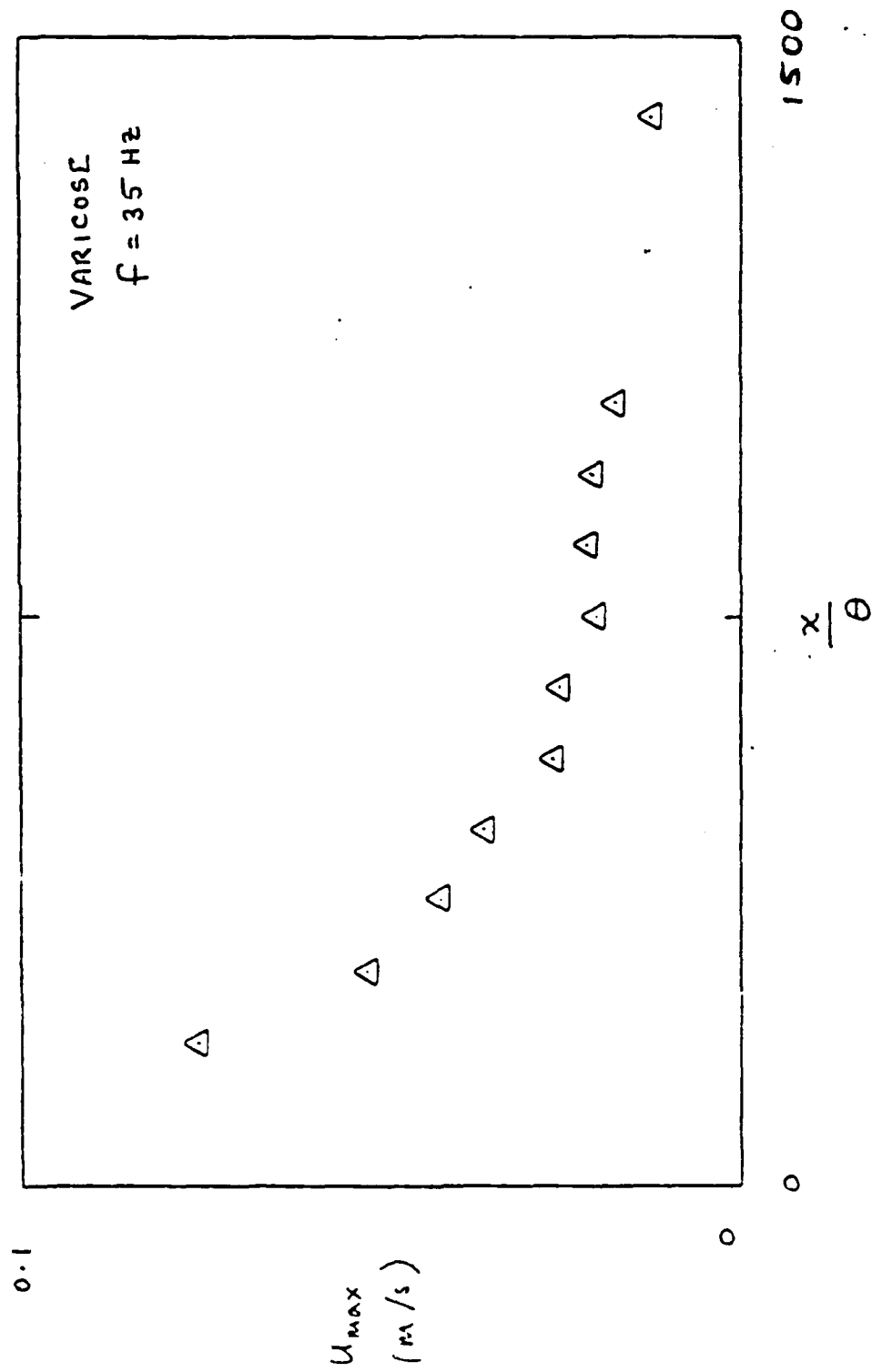
8

FIGURE 5: The downstream variation of maximum amplitude.

9

asymmetries which might be present in the experiments. As the amplification rates of the antisymmetric sinuous mode are much larger than those for the symmetric varicose mode, these asymmetries are preferentially amplified resulting in the eventual destruction of an initially prominent symmetric wave. It was evident, therefore, that the total phase averaged signal should be decomposed into its symmetric and antisymmetric modes in order to study their downstream evolution.

DECOMPOSITION PROCEDURE

To decompose the phase averaged data into modes, we will take advantage of the fact that the sinuous and varicose modes are odd and even functions of y, respectively, for the u component of the velocity perturbations. Therefore, if we separate the measured perturbations into odd and even parts, we may have a means of separating the sinuous and varicose modes. The amplitude and phase distribution of the separated parts would then have to be examined and compared to the theoretical distributions of the sinuous and varicose modes.

The decomposition procedure gives as follows. First, we measured the lateral distribution of the phase averaged u component using an array of nine hot wires. Typically, 36 points were used to define a distribution. The phase averaged data for each y position was Fourier transformed to determine u_f, the u component of the velocity perturbation associated with the forced wave at the forcing frequency. The lateral distribution of the real and imaginary parts of u_f are shown in the upper plots of Figure 6, for some example data. The triangles and squares represent the data. The
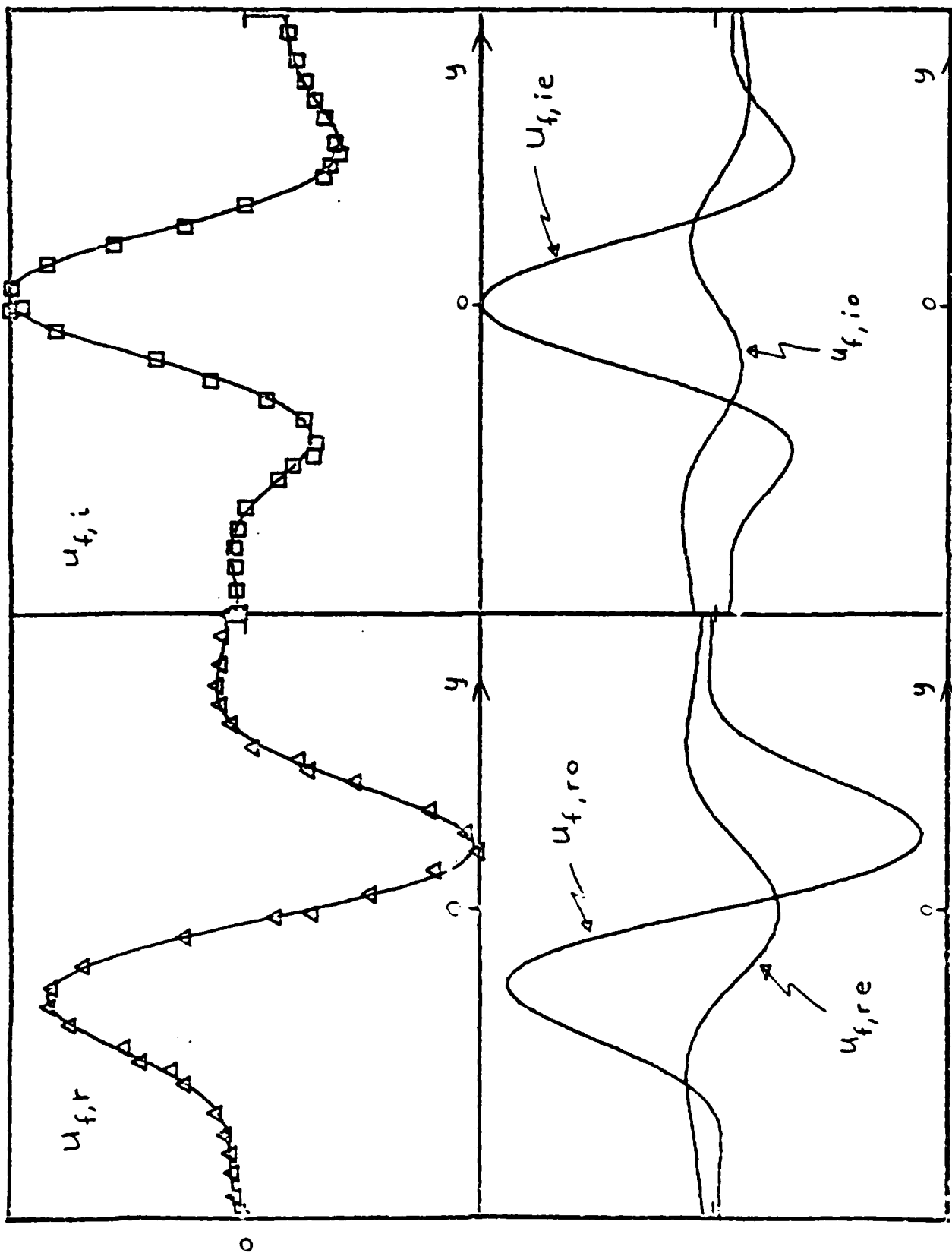
FIGURE 6: Decomposition of phase averaged distribution into odd and even parts.

11

scales of the ordinates for $u_{f,r}$ and $u_{f,i}$ are not the same. The subscripts r and i represent real and imaginary, respectively. The absiccas are all y with ranges $-4L_0$ to $+4L_0$. Then, to obtain the odd and even parts, the location of the wake centerline, $y=0$, was established from mean velocity measurements. Next, as we generally did not have data at exactly the same $\pm$ y locations, we fit a curve to the measured data. A Fourier series in y was fit to the real and imaginary parts separately. The fit curves are shown by the solid lines. The Fourier series fit to each was separated into its odd and even parts shown in the lower plots of Figure 6. The odd and even parts or modes were then formed according to

$$u_{f,e} = u_{f,re} + iu_{f,re}$$

$$u_{f,o} = u_{f,ro} + iu_{f,ro}$$

where the subscripts o and e refer to odd and even, respectively. The lateral distributions of the magnitude and phase of the odd and even modes were then determined and plotted. The results for the example data are shown in the plots of Figure 7. Next, a check was performed on the results. From the measured data, we determined the magnitude and phase angle of u_f for each measurement location y, shown by the triangles and squares in the upper plots of Figure 7. Then, we estimated the same distribution from the curve fits to the real and imaginary parts. The results, shown by the solid lines, agree well with the data. Note, for the example data, the amplitude distribution has a large even component although it is asymmetric.
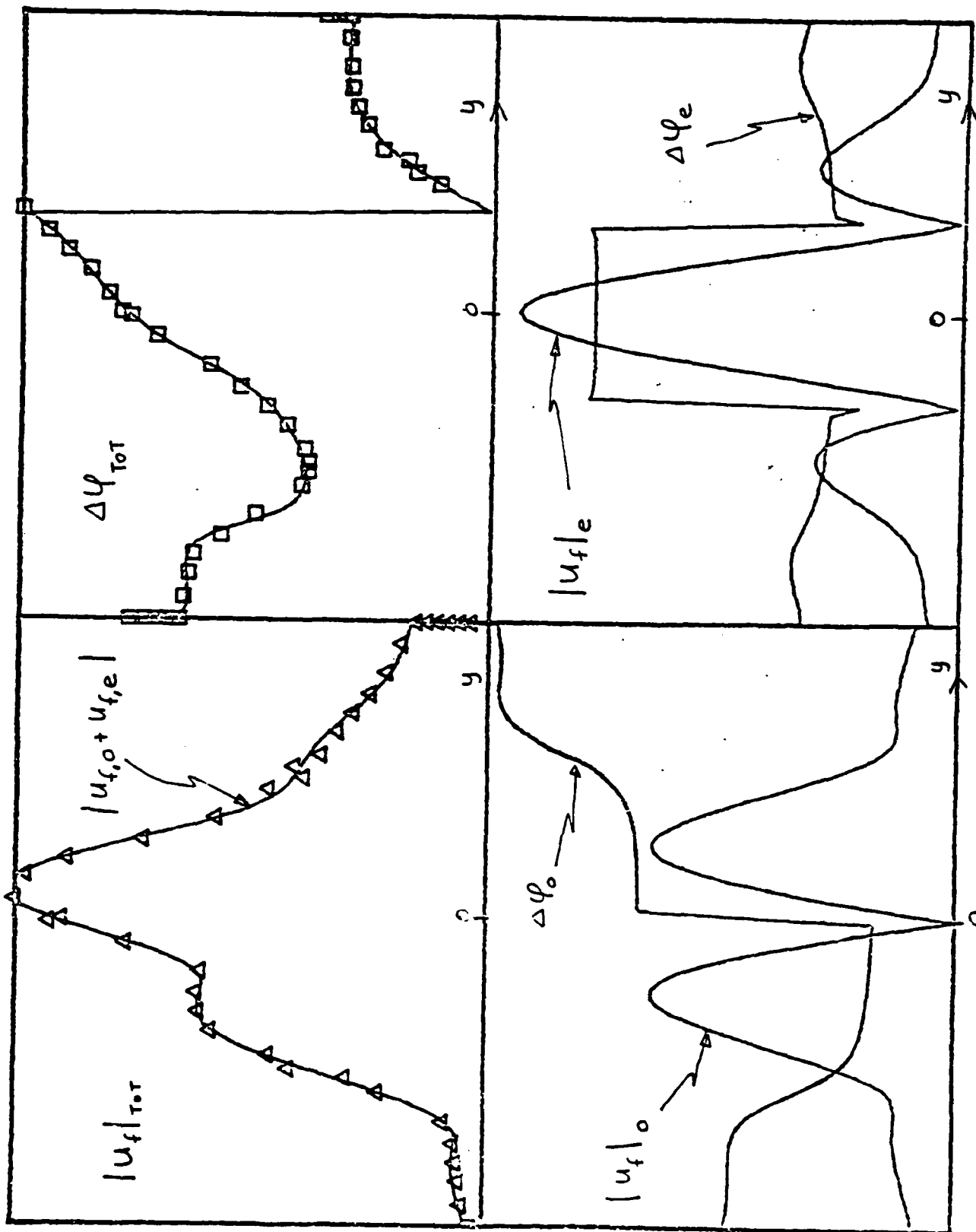
FIGURE 7: Decomposition Plots.

COMBINED MODEL FORCING OF WAKE

By applying a small phase difference to the relative motion of the two flaps, a sinuous component was also introduced. This provides a means of simultaneously forcing the wake with both modes to study their interaction. The results of combined forcing at a frequency of 28 Hz in terms of the lateral distributions of $\overline{u^2}/u_0^2$ are shown in Figure 8. The flow is self preserving, but the $\overline{u^2}$ distribution is asymmetric. The asymmetry depends on the phase relationships between the modes.

The measured amplitude and phase distribution of u_f for five downstream locations is shown in Figure 9. Each plot is displaced vertically for display purposes. The ordinate for each is the dimensional amplitude of u_f. The absicca is y and in the same scale for each plot. The wake growth with x is evident. The amount of asymmetry changes with x but appears to remain nearly constant in the far wake. These distributions, were plotted in terms of their real and imaginary parts and then decomposed into the odd and even parts. The resulting odd part for each downstream location is plotted in Figure 10(a), designated by transfer. The ordinate is the dimensional amplitude and the absicca is y again. The solid lines represent the amplitude of the theoretical sinuous mode computed from linear, inviscid stability theory, using the measured men velocity profiles. The amplitude of the theoretical sinuous mode was adjusted by a constant determined by matching the integral under the theoretical curve to that under the measured data. The comparison between the theoretical and measured phases is shown in Figure 10(b). The agreement between the measured odd parts and the theoretical sinuous mode is
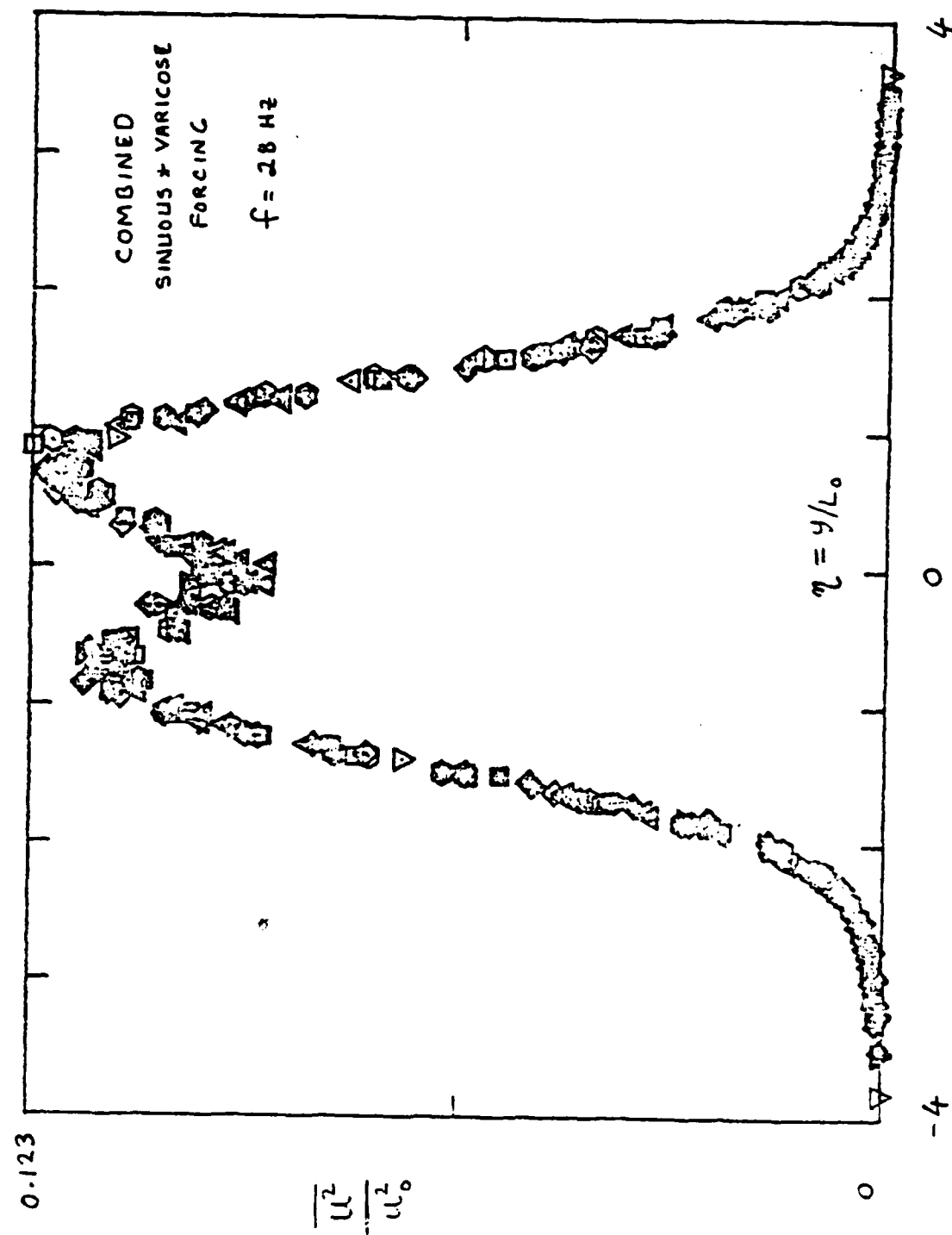
14

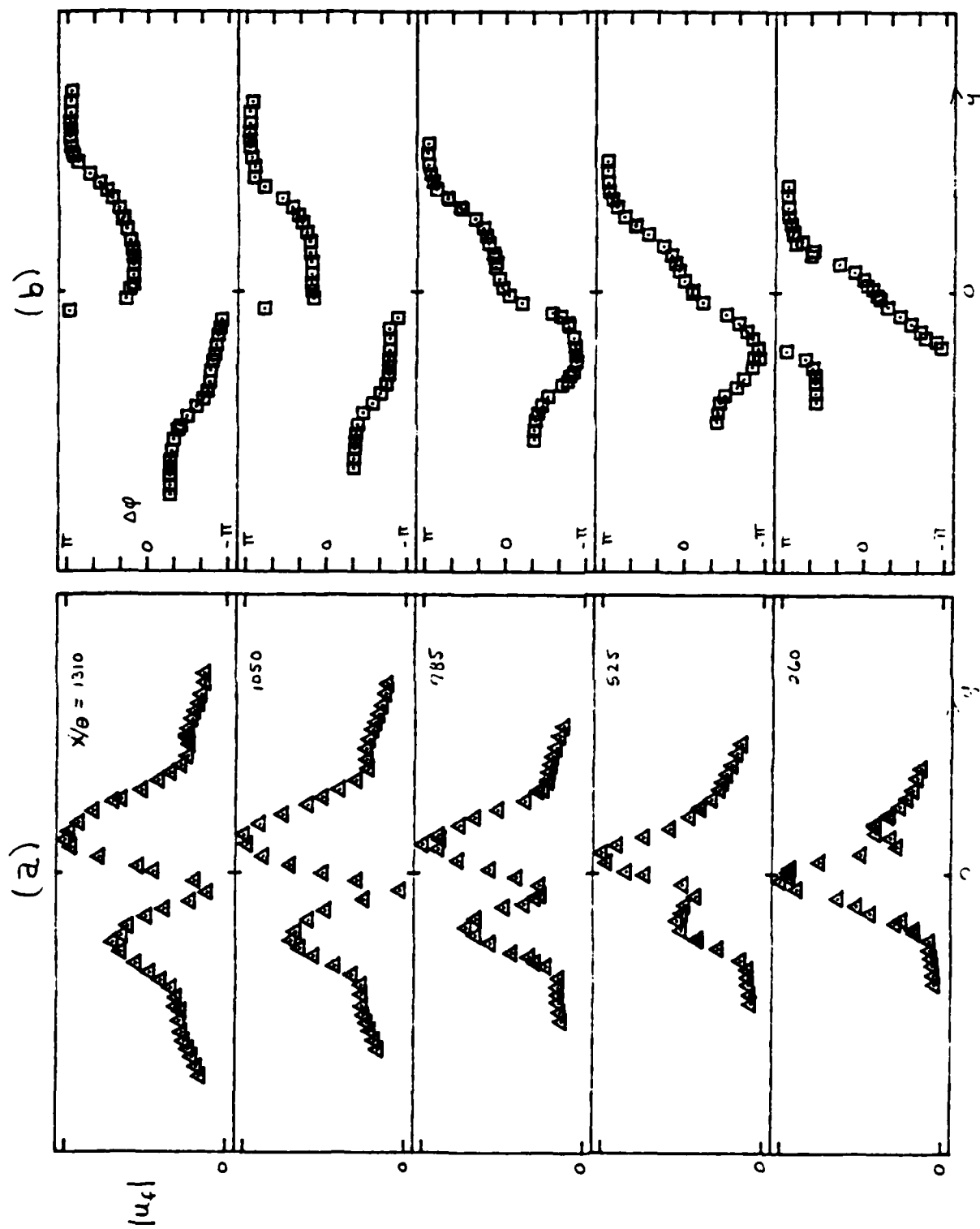FIGURE 8: The measured distributions of $\overline{u^2}/u_o^2$ for forced wake.

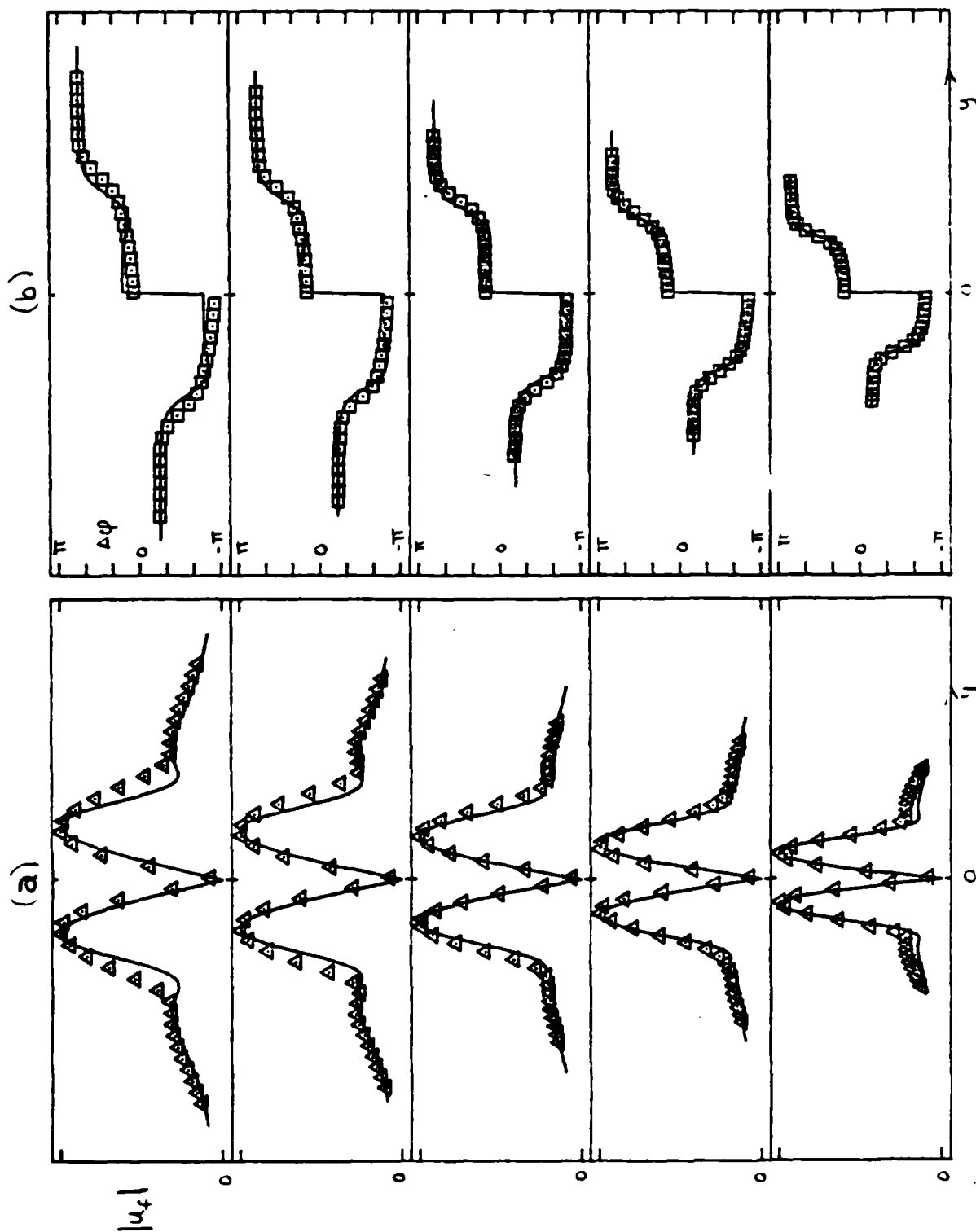FIGURE 9: The measured amplitude and phase distribution of the forced wave.

16

FIGURE 10(a): The amplitude distributions of the antisymmetric component; Δ, measured; ——, theoretical sinuous.

FIGURE 10(b): The phase distribution of the antisymmetric component; □ measured; ——, theoretical sinuous.

17

quite good.   Thus the measured odd part undoubtedly corresponds to the sinuous mode of linear, stability theory.

The amplitude and phase distribution for the even parts for each downstream location are shown in Figure 11(a) and (b). The solid lines represent the theoretical varicose distributions where again the amplitude was adjusted by a constant determined by matching the integral under the thoeretical curve to that under the measured data. The agreement is quite satisfactory and the even part indeed corresponds to the varicose mode of linear stability theory.

The relative intensity of the two modes was obtained by integrating the amplitude distributions across the flow for each mode and taking the ratio of the two. The downstream evolution of the ratio is shown in Figure 12.   Initially, the amplitude of the varicose mode is about twice that of the sinuous mode, but in accordance with linear theory the sinuous mode eventually dominates and an equilibrium ratio is reached for x/Θ >1000, at least for this particular experiment.
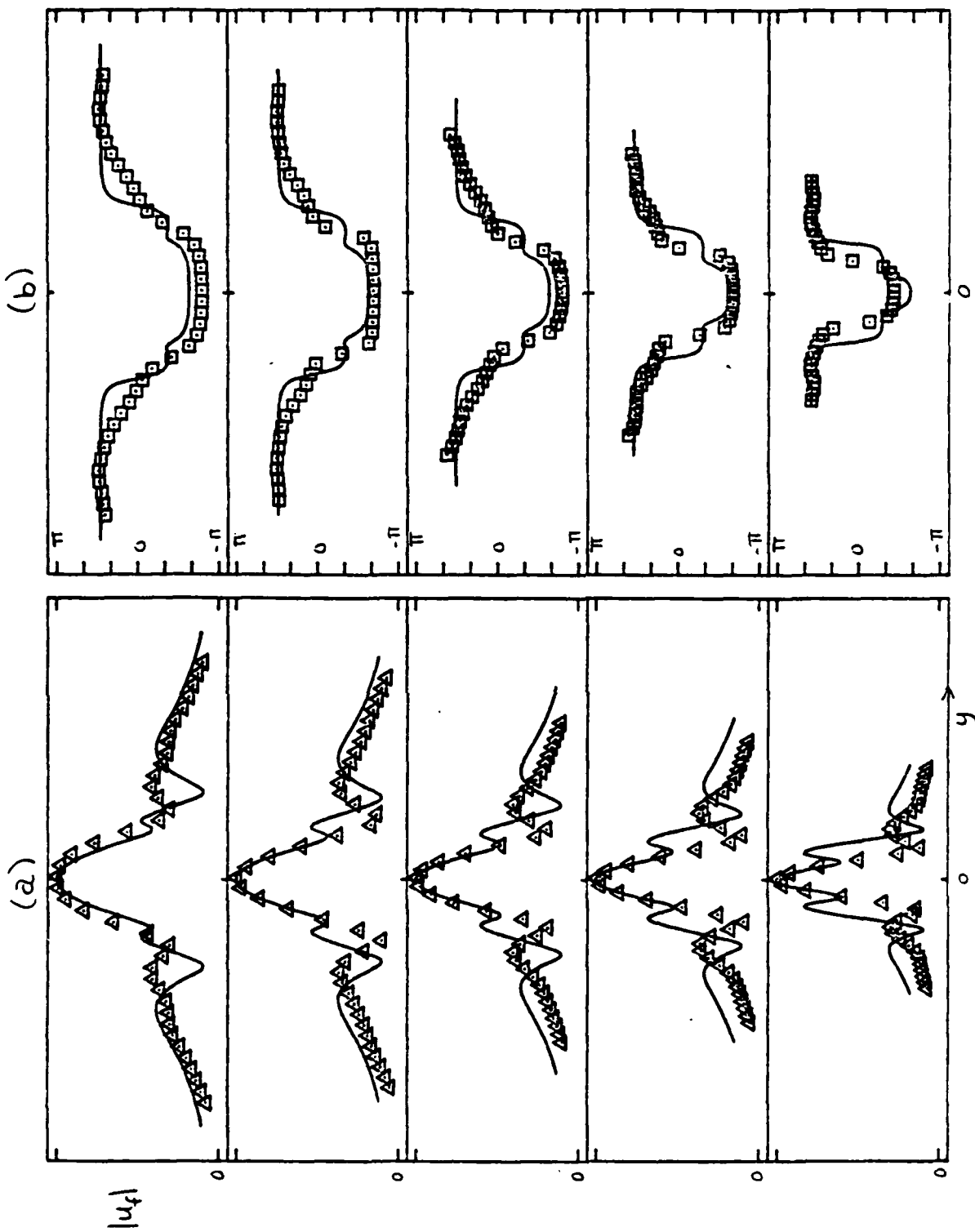
FIGURE 11(a): The amplitude distribution of the symmetric component; Δ, measured; ——, theoretical varicose.

FIGURE 11(b): The phase distributions of the antisymmetric component; □, measured; ——, theoretical varicose.
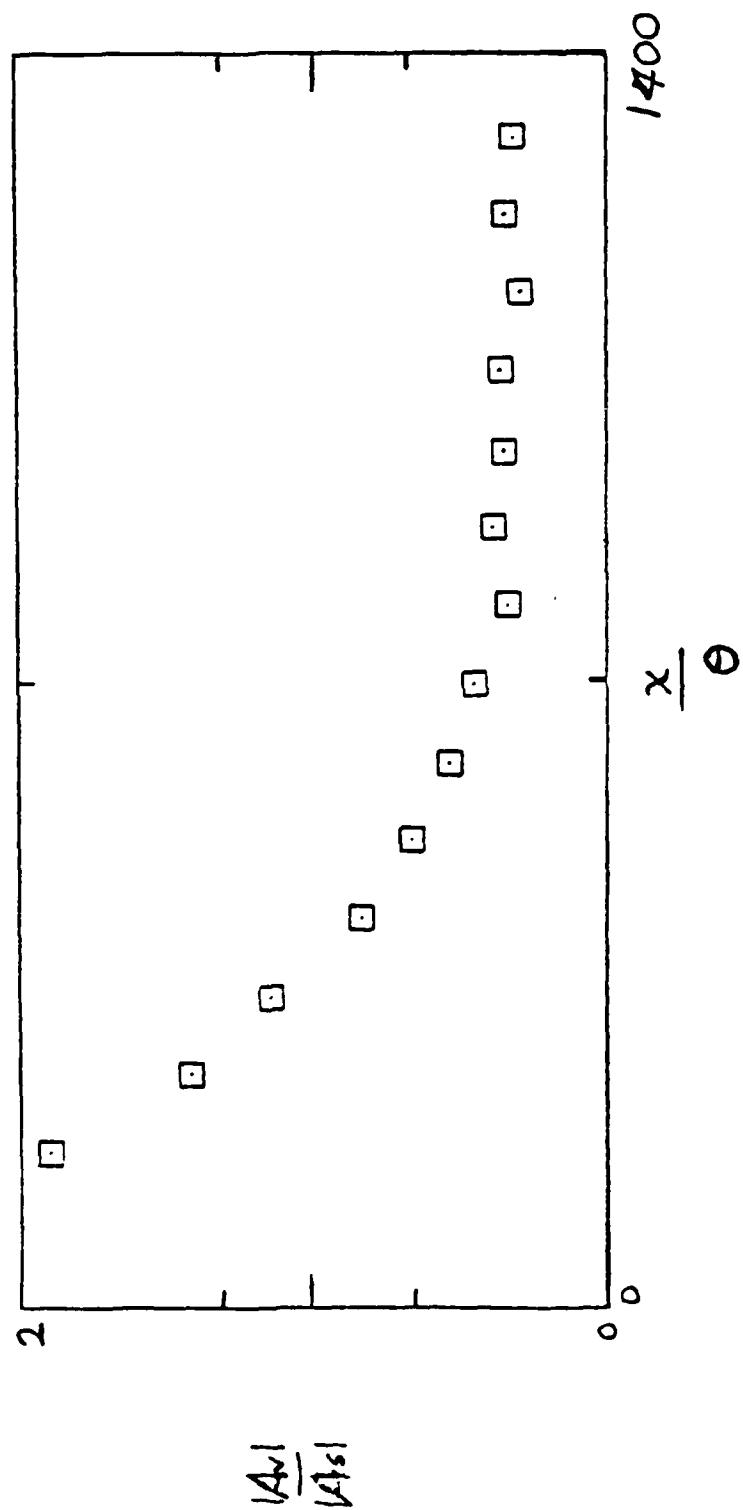
FIGURE 12: The relative ratio of modes, varicose to sinuous.

CONCLUSIONS

It is possible to generate a nearly pure varicose mode of instability in the wake. The sensitivity of the flow to asymmetric disturbances, however, makes it a difficult experimental task. Even the slightest asymmetric disturbance can be preferentially amplified as the growth rates of sinuous disturbances are much larger than those for varicose disturbances. Therefore, contamination of the varicose mode by the sinuous mode is difficult to avoid, especially over large downstream distances.

A decomposition technique was developed to separate a phase averaged distribution into its symmetric and antisymmetric components. The measurements show that these components agree well with their corresponding theoretical counterparts, that is, the varicose and sinuous modes from linear stability theory. The relative strength of the two modes at any downstream location can then be determined by integrating the amplitude distribution across the flow for each mode and taking the ratio of the two. The model decomposition technique was applied to a case of combined excitation. The relative strength ratio measurements show that initially the varicose mode was twice as strong as the sinuous mode, but the sinuous mode eventually became dominant because of the larger amplification rates. An equilibrium ratio was approached in the far wake for $x/\Theta > 1000$.

21

REFERENCES

Betchov, R. and Criminale, W. O., 1967, Stability of Parallel Flows, Academic Press.

Papailiuou, D. D. and Lykoudis, P. S., 1974, "Turbulent Vortex Streets and the Entrainment Mechanism in the Turbulent Wake," J.F.M. 62, 11-31.

Wygnanski, I. J., Champagne, F. H. and Marasli, B., "On Large Scale Structures in Two-Dimensional, Small-Deficit, Turbulent Wakes," accepted for publication in Journal of Fluid Mechanics, 1985.

END

5-81

DTIC